≪연구논문≫ Journal of The Korean Magnetics Society, Volume 15, Number 2, April 2005

Mössbauer Analysis of Cations on Iron Oxyhydroxide Formation

Sei-Jin Oh*

Department of Acoustics, JuSung College NaeSoo-Ub ChengWon-Kun ChungBuk 363-794

Soon-Ju Kwon

Department of Materials Science and Engineering Pohang University of Science and Technology PohangSi KyoungBuk 790-784

(Received 22 February 2005, in final form 4 March 2005)

Effect of different cations to the formation of iron oxyhydroxide was studied using Mössbauer spectroscopy, X-ray diffraction (XRD) and BET. Redox Potential and pH were measured for the determination of the internal reaction rate, as well. The phases of iron oxyhydroxide could not be the same with each other, due to the presence of different cations in solution. Although the oxyhydroxide compound was composed of the same phases, the fraction of each phase was different from each other. The internal reaction rate was varied by the substitution of cation. It could be a cause of the different phase and particle size of oxyhydroxide compound.

Key words : Cation, Iron Oxyhydroxide, Internal Reaction Rate, Redox Potential, Mössbauer Spectroscopy

I. Introduction

Corrosion properties for steel structures can be varied by environmental condition and kind of steel [1-5]. For example, the corrosion rate of steel structure which is exposed at rural site, is generally lower than them for industrial and marine sites. As well as, lepidocrocite (γ-FeOOH) frequently forms on the steel surfaces which are located at rural and industrial sites, while akaganite (β-FeOOH) forms on it at marine site. The formation of akaganite at the marine, which is closely related to the presence of Cl^- in the environment, can become a cause of increasing the corrosion rate of steel [5]. The corrosion behavior can be also changed by the kind of steel under the same exposure condition [1-5]. For example, the resistance of weathering steel against the atmospheric corrosion is generally higher than that for carbon steel [1-15]. The reason is that a protective layer is formed on the surface of weathering steel. The protective layer on the weathering steel is composed of very fine goethite (α-FeOOH) particles, which are closely caused by the presence of cations in the steel substrate [3]. Therefore, studying the effect of cations to the formation of iron oxyhydroxide and oxide should be very important for understanding the atmospheric corrosion behavior of the steel structures.

In this study, the effect of nine cations on the formation of iron oxyhydroxide is investigated with their substitution in the corrosive solution. The results will be possible to achieve a better understanding of the corrosion behavior under the environmental or the steel condition to be contained these cations. They can be also used for good information to form the complete protective layer on the surface of weathering steel, in order to improve the resistance against atmospheric corrosion.

II. Experimental Procedure

After mixing two solutions of tetrahydrate ferrous chloride ($FeCl_24H_2O$, 99.99 %) and caustic soda (NaOH) in a reactor, the mixed solution containing ferrous sulphate and ferrous chloride ions was stirred. The equations of chemical reaction are as below:

$$FeCl_2+2NaOH=Fe(OH)_2+2NaCl$$
$$4Fe(OH)_2+O_2=4FeOOH+2H_2O.$$

Then, the ferric Fe^{3+} ions would be included in tetrahydrate ferrous chloride, and also produced by the oxidation of ferrous Fe^{2+} ions during substituting it into the solution. By substituting the iron powder into the $FeCl_24H_2O$ solution, which is called as a method of cementation reaction [16], all ferric Fe^{3+} ions existing in the solution

*Tel: (043) 210-8336, E-mail: seijin@jsc.ac.kr

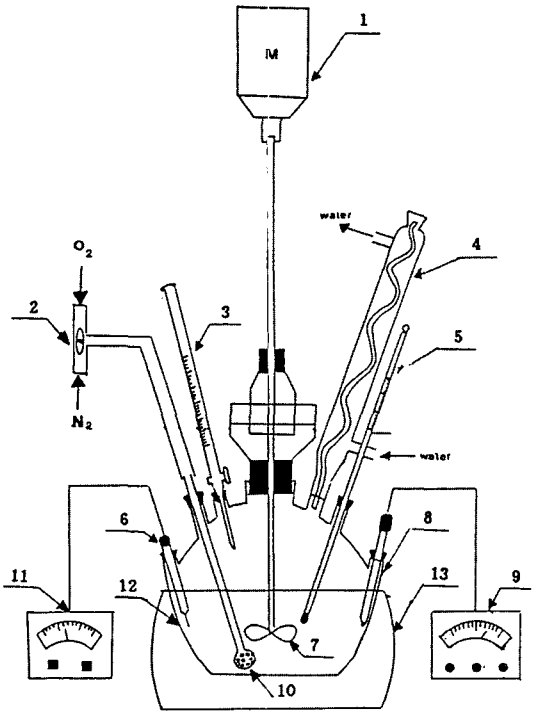

1. Motor 2. 3-way valve 3.Buret 4.Reflux condenser 5. Thermometer
6. Pt-Calomel electrode 7. Stirrer 8. Glass electrode 9. pH meter
10. Gas distributer 11. Potential meter 12. Reaction vessel 13. Heating mantle

Fig. 1. Apparatus for the sample fabrication in this experiment.

were reduced to the ferrous Fe^{2+} ions, as below:

$2FeCl_3+Fe=3FeCl_2$.

After removing the iron powder by a filter, the pure $FeCl_2$ solution without the presence of ferric Fe^{3+} ions was mixed with the NaOH solution.

The $FeCl_2$ and NaOH solutions and the cation were mixed at the reactor, as shown in Fig. 1. Of the 1.6 mol tetrahydrate ferrous chloride in one liter, 0.1 mol was replaced by the cation. The chemical reagent of the cation to be used for this study is shown in Table I, and the weight percentage about each cation is indicated in Table II. For performing all experiments, R.P.M. of stirrer was 1750, and the flow rate of bubbling gas, air, flowing in the

Table I. The chemical reagent of cation.

Cation	Atomic number	Chemical reagent	Cation	Atomic number	Chemical reagent
Mg	12	$Mg(OH)_2$	Ca	20	$Ca(OH)_2$
Al	13	$AlCl_3$	Cr	24	$CrCl_3$
Si	14	$xNa_2OySiO_2zH_2O$	Mn	25	$MnCl_2$
P	15	H_3PO_3	Ni	28	$NiCl_2$
Cu	29	$CuCl_2$			

Table II. Weight percent (%) of cation relative to 0.1 mol per one liter.

Cation	Atomic number	Weight percent	Cation	Atomic number	Weight percent
Mg	12	6	Ca	20	13
Al	13	7	Cr	24	14
Si	14	7	Mn	25	15
P	15	8	Ni	28	16
Cu	29	10			

solution was 2 liter/min. Before starting the chemical reaction, the N_2 gas was flowed in the solution in order to prohibit the oxidation of ferrous Fe^{2+} ions. The initial temperature of the solution was about 25°C, and the ratio, $2\times[Cl^-]/[OH]$, between Cl^- and OH ions was always 0.3125. During the chemical reaction, pH and redox potential were respectively measured by means of saturated calomel electrodes, a platinum electrode and a thermocouple, and were recorded by on-line computer program. During completely finishing the oxidation reaction of ferrous Fe^{2+} ions present in the mixed solution, recording the variations of pH and redox potential allowed to characterize each stage where the different products was precipitated. The determination of reaction time indicating the end of all oxidation reaction allowed to calculate the internal reaction rate, as previously defined by Lee [17]:

Internal Reaction Rate
=mols of final products/(the reaction time×volume)

where the units for the final products, the reaction time and volume were millimols, minute and liter, respectively. In this study, the amount of final products was fixed as 0.25 mols per one liter. By the comparison of internal reaction rate about each cation, a correlation between the kinetics and the formation of final products was obtained.

When all chemical reaction completely finished, the final product was immediately removed from the solution, washed, filtered and dried. In order to identify the phase of the final product, they were qualitatively analyzed by XRD using CuK_α radiation. After accurately prepared to a mass of 13 mg, they were uniformly dispersed with boron nitride, and were pressed into a 8 mm diameter tablet. Their transmission Mössbauer spectra were recorded at 300 K and 77 K using a 48 mCi ^{57}Co source in rhodium matrix, operating in a triangular wave motion. After the experimental data were fitted by a superposition of sextets and doublets, the 300 K and 77 K fit parameters were compared to them for the standard oxyhydroxide samples published [3], in order to identify the phase of the final products. With the complete fit of Mössbauer spectra, the fraction of each phase consisting of the final products

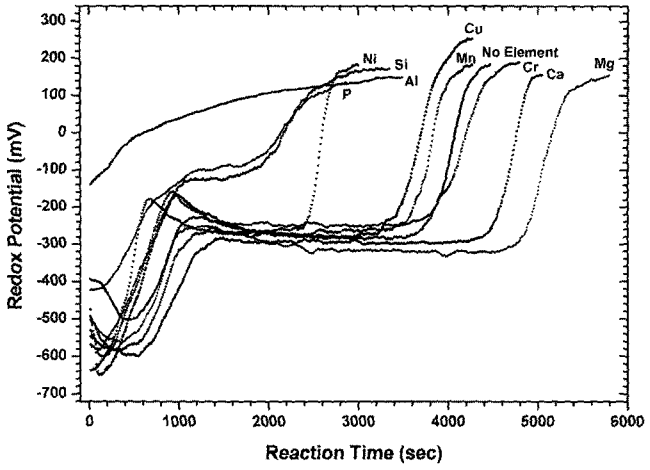

Fig. 2. The redox Potential behavior due to the substitution of cation.

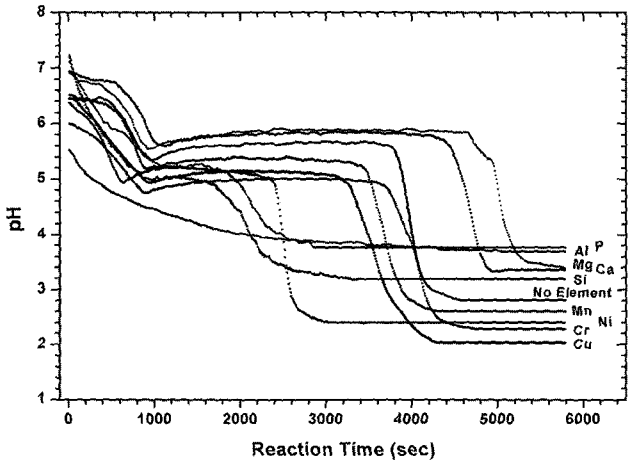

Fig. 3. The pH behavior due to the substitution of cation.

was quantitatively determined. The particle size and the average surface area of the final products were analyzed by BET.

III. Results

3.1. Analysis of Redox Potential

With substituting the cation, the variation of redox potential and pH are respectively shown in Fig. 2 and 3. Except for the Al substitution, the redox potential and pH curves are overall similar to each other, but the reaction

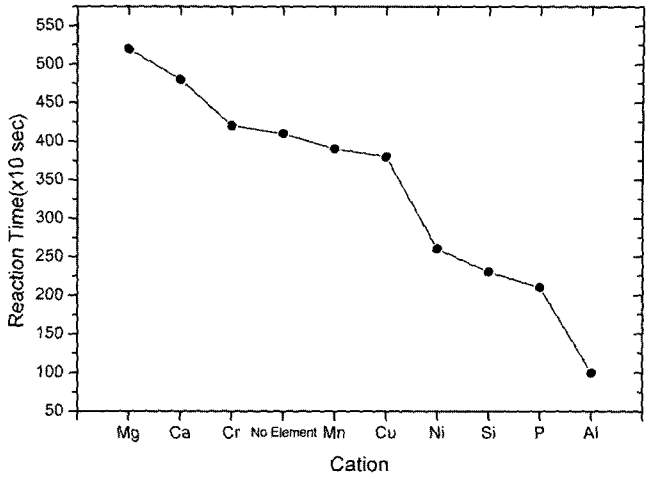

Fig. 4. The reaction time as a function of cation.

time are not the same (Fig. 4). Table III indicates that the internal reaction rates for the Mn and Cr substitution were not much different from the case of "no element" that nothing was substituted into the solution. This means that the internal reaction rate was not varied by the presence of Mn and Cr in the corrosive solution. The substitution of Ca and Mg was a cause of the reduction of the internal reaction rate, as listed in Table III. However, the substitution of Cu, Al, Ni, P and Si into the solution increased it. In particular, the increase of internal reaction rates for P, Si and Al were very large. As a result of the increase, the redox potential and pH curves for the substitution of Al were very different from the others. It means that the stages representing the formation of Green Rust I and oxyhydroxide were not distinctly separated from each other, because the reaction was performed too fast. The XRD, Mössbauer and BET analysis will allow to discuss the effect of different internal reaction rates to the oxyhydroxide formation.

3.2. XRD Analysis

As shown in Fig. 5(a), it appears that the final products for the case of "no element" were composed of lepidcrocite, as well as small amount of akaganite and goethite (Table IV). The XRD spectrum was very similar to Fig. 5(b) that Mg was substituted in the solution. However, Fig. 5(c)-(e), which are exhibiting the substitution of Al, Si and P, are very different from Fig. 5(a). It implies that the

Table III. The variation of internal reaction rate (millimol/liter^{-1} min.$^{-1}$) as a function of cation.

Cation	No element	Mg	Al	Si	P	Ca	Cr	Mn	Ni	Cu
Atomic number		12	13	14	15	20	24	25	28	29
Internal reaction rate	3.66	2.88	15.0	6.52	7.14	3.95	3.57	3.85	5.77	3.13

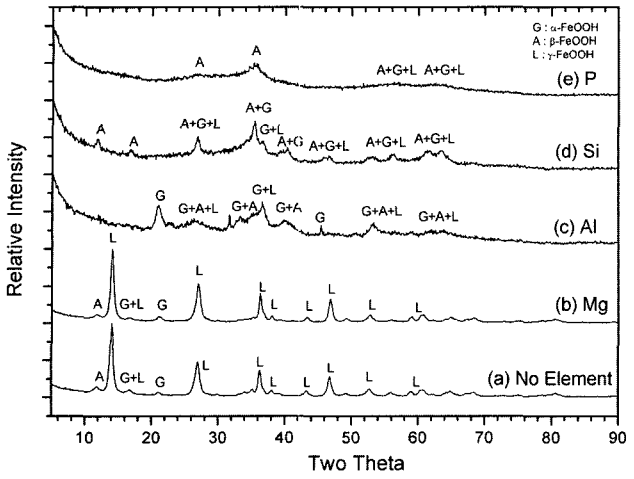

Fig. 5. The XRD analysis of iron oxyhydroxides substituted with Mg, Al, Si, and P.

final products could be composed of amorphous or fine particles, because the linewidth of peaks were very large. The peak broadening did not allow the unique separation of peaks of minor phase from main one. For example, with substituting the Al cation in the solution, the dominant phase for the final products was goethite, and small amount of akaganite and lepidocrocite could also exist in the final products (Table IV). The reason is that the peaks to be caused small amount of akaganite and lepidocrocite could not be distinctly identified from the broaden peaks for goethite. When Si and P were substituted into the solution, the final products were consisted of akaganite, but small amount of goethite and lepidocrocite might be in the products (Table IV). It is the reason that if the amount of goethite and lepidocrocite were very small, their peaks would not be separated from the broaden peaks of akaganite. Fig. 6 shows that the XRD spectra for Ca, Cr, Mn, Ni and Cu are closer to the case of "no element". It appears that the final products for Ca, Cr, Mn and Ni were pure lepidocrocite (Table IV).

Table IV. The XRD analysis of final products as a function of cation.

Cation	No element	Mg	Al	Si	P	Ca	Cr	Mn	Ni	Cu
α-FeOOH	○	○	○	△	△	○	○	×	○	○
β-FeOOH	○	○	△	○	○	○	○	○	○	○
β-FeOOH	○	○	△	△	△	○	○	○	○	○

○: Presence, △: possible, ×: No Presence.

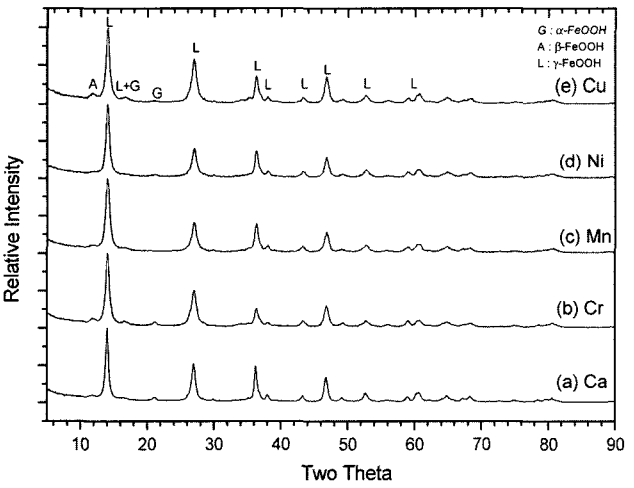

Fig. 6. The XRD analysis of iron oxyhydroxides substituted with Ca, Cr, Mn, Ni and Cu.

3.3. Mössbauer Analysis

Fig. 7(a) and (g) are the 300 K and 77 K Mössbauer spectra for the case of "no element". They are composed of the doublet which indicates the non-magnetic material, and sextet which means the magnetic one. For the 300 K Mössbauer spectrum (Fig. 7(a)), the sextet is corresponding to goethite, while the doublet is akaganite, lepidocrocite and/or the mixture of akaganite and lepidocrocite. Akaganite and lepidocrocite were not uniquely separated at the room

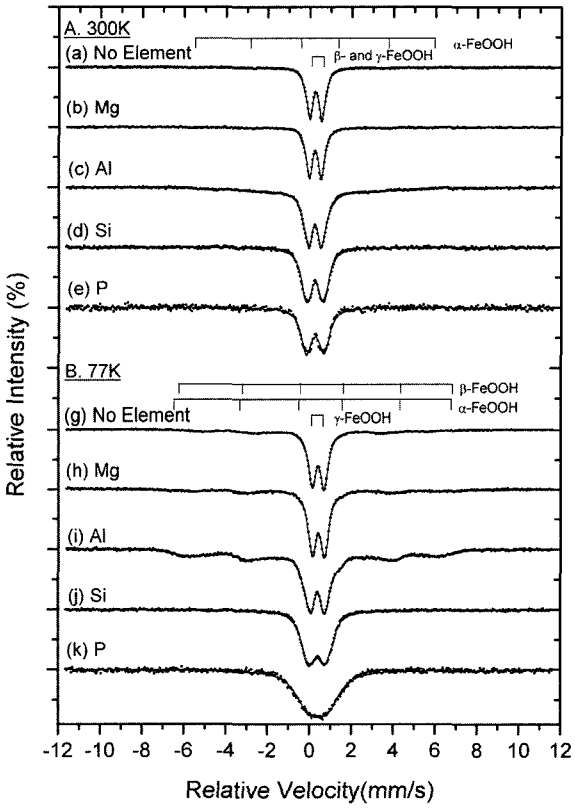

Fig. 7. The Mossbauer analysis of iron oxyhydroxides substituted with Mg, Al, Si, and P.

temperature, because their Mössbauer parameters were almost the same with each other [3]. However, the doublet representing akaganite at 300 K revealed to the sextet at 77 K because it was below the Neel temperature (about 270 K) of akaganite. However, the spectrum for lepidocrocite represented still doublet at 77 K. Therefore, these phases should be uniquely separated from each other at 77 K (Fig. 7(g) and Table V). In Fig. 7(g), the doublet is corresponding to pure lepidocrocite, while the sextet is the mixture of goethite and akaganite phases. The Mössbauer quantitative analysis for the case of "no element" is listed in Table V.

The Mössbauer spectra for Mg, Al, Si and P are also composed of the doublet and sextet, as shown in Fig. 7(b)-(e) and 7(h)-(k). These Mössbauer spectra are similar to those for the case of "no element". However, the values of quadrupole splitting and linewidth for the doublet increased from Fig. 7(a) to Fig. 7(e) at 300 K, and from Fig. 7(g) to Fig. 7(k) at 77 K. This implies that the amount of amorphous particles in the final products gradually increased. It is also possible for the particle size to be decreased. This is the reason that akaganite, which was already confirmed by the XRD analysis, was not uniquely identified in the 77 K Mössbauer spectra for the Si and P cations. However, the linewidth of doublet was broadened. Therefore, the final products would be consisted of the fine akaganite, which could exhibit the superparamagnetism at 77 K. The Mössbauer quantitative analysis for the Mg, Al, Si and P substitution is appeared in Table V.

Fig. 8 shows the 300 K and 77 K Mössbauer spectra for the Ca, Cr, Mn, Ni and Cu substitution. These Mössbauer spectra are closer to those, Fig. 7(a) and (g), for the case of "no element". This implies that the phases, which are composed of these final products, are similar to each other in spite of the substitution of different cations. However, Table V shows the Mössbauer analysis that the phase fraction of final products depended on the substitution of different cation.

3.4. Analysis of BET

It is shown from XRD and Mössbauer analysis that the different phase and particle size of final products resulted from the internal reaction rate due to the substitution of cation. The relationship between the variations of internal

Table V. The Mössbauer analysis of final products as a function of cation.

Cation	No element	Mg	Al	Si	P	Ca	Cr	Mn	Ni	Cu
α-FeOOH	5	10	61	7	5	8	11	0	4	5
β-FeOOH	21	15	26	85	91	10	13	10	7	14
γ-FeOOH	74	75	13	8	4	82	76	90	89	81

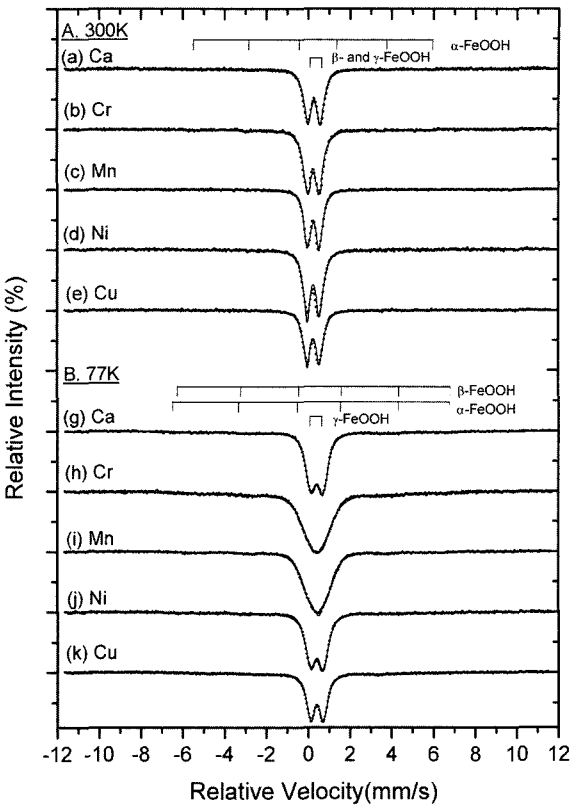

Fig. 8. The Mossbauer analysis of iron oxyhydroxides substituted with Ca, Cr, Mn, Ni and Cu.

Table VI. The average surface area of final products by BET.

Cation	Al	No element	Si	P	Ni
Atomic number	13		14	15	28
Average surface area	2.85	71.18	217.16	238.81	79.05

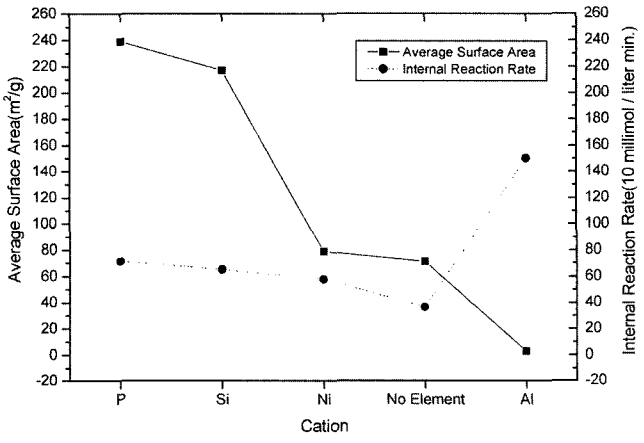

Fig. 9. The reaction rate and the average surface area of oxyhydroxide substituted P, Si, Ni, and Al.

reaction rate and average surface area to be obtained by the BET analysis is presented in Table VI and Fig. 9. The average surface area for the Ni, Si and P substitution was larger than that for the case of "no element". It implies that the increase of average surface area can be conversely meant the reduction of average particle size. This is the reason that the ferrous Fe^{2+} ions in the solution did not consume for increasing the number of oxyhydroxide, but for growing the crystal. The particle size for the Al substitution was the largest of the other final products (Table VI).

IV. Discussion

As shown in Fig. 10, the final products were different from each other, according to the substitution of cations. In detail, although the phases of final products were the exactly same, the phase fraction was different from each other. All final products, except for the Mn substitution, were composed of lepidocrocite, akaganite and goethite. When Ni and Mn were substituted into the solution, the fraction of lepidocrocite increased from 74 % to 89 % and 90 %, respectively. 7~8 % of lepidocrocite reduced with the Ca and Cu substitution, while it was not varied with the Mg and Cr substitution. However, when P, Si and Al were added in the solution, 4 %, 8 % and 13 % of lepidocrocite decreased in the final products, respectively. This could be related to the variation of internal reaction rate (Fig. 11).

Comparing to the case of "no element", the internal reaction rates for the Si, P and Al substitution respectively increased from 3.66 to 6.52, 7.14 and 15.0, as shown in Fig. 11. This did not result in the formation of lepidocrocite, but akaganite and goethite. With the P and Si substitution, the fraction of akaganite in the final products increased

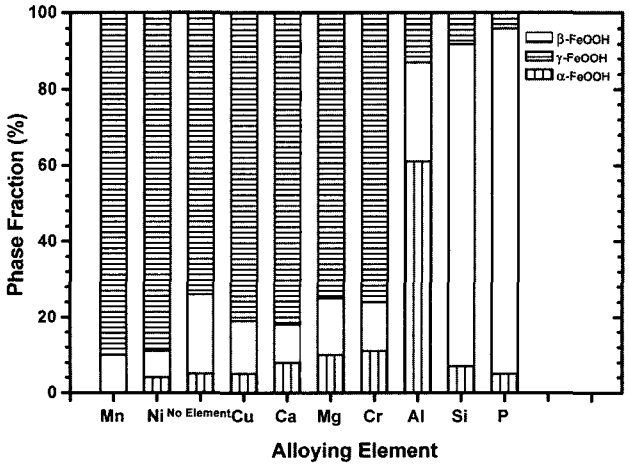

Fig. 10. The Mossbauer analysis as a function of cation.

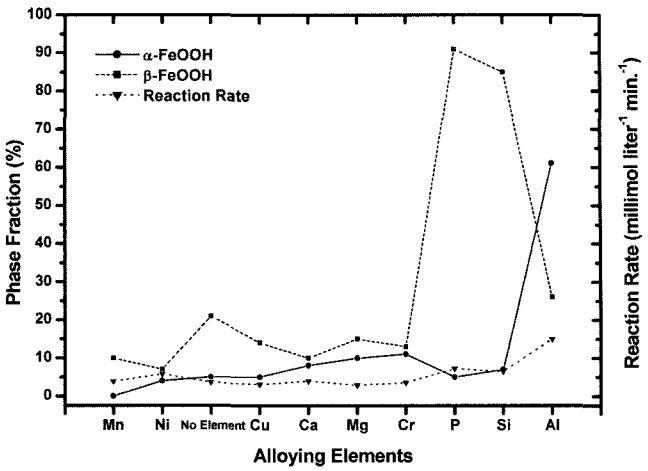

Fig. 11. The reaction rate and the Mossbauer analysis as a function of cation.

from 21 % to 91 % and 64 %, respectively. The reason is that although akaganite generally formed by the slow oxidation of ferrous Fe^{2+} ions in the Cl^- solution, it is possibly formed by their very fast oxidation. The Cl^- ions could not escape from Green Rust I during the transformation of Green Rust I into FeOOH, because the ferrous Fe^{2+} ions in the solution were oxidized too fast. This finally resulted in the formation of akaganite. However, although the internal reaction rate for the Al substitution was much higher than those for the P and Si substitution, goethite dominantly formed in the final products instead of akaganite. The exact reason has not been figured out until now, but it will be a topic for a further research. In general, the fraction of akaganite decreased due to substituting cation into the solution, such as Mg, Cu, Cr, Ca, Mn and Ni. In the Ni case, the fraction of akaganite reduced from 21 % to 7 %. This could be resulted from the reason that some of Cl^- ions in the solution consumed for the formation of $Fe_{7.6}Ni_{0.4}O_{6.35}(OH)_{9.65}Cl_{1.25}$ [10].

In Fig. 10, the substitution of Mn completely prohibited the goethite formation, while the fraction of goethite for the Ni, Cu, P and Si substitution was very similar to that for the case of "no element". However, the substitution of Ca and Mg was a cause of increasing pH in the solution (Fig. 3), and increased the fraction of goethite from 5 % to 8 % and 10 %, respectively. It is already discussed in the other paper by these authors that the formation of goethite very enforced in the alkali environment and the substitution of Cr in the corrosive condition [11, 13-14]. The effect of Cr has been investigated for the completely formation of protective layer on the surface of weathering steel [11, 13-15]. In detail, the Cr ions densely distributed in the protective layer, which formed with the fine goethite, α-$(Fe_x, Cr_{1-x})OOH$, [11, 13-15].

V. Conclusion

The effect of cation to the formation of oxyhydroxide in the corrosive solution is as below:

(1) The Mn, Ni, and Cu cations were helpful for forming lepidocrocite, but they reduced the amount of goethite and akaganite,

(2) the substitution of Mg and Ca enforced the formation of goethite with increasing pH of the solution,

(3) when Al and Cr were substituted in the solution, the amount of goethite was the largest of all substitution,

(4) the substitution of P and Si increased the internal reaction rate and the amount of akaganite, but they decreased the average particle size,

and (5) the decrease of lepidocrocite was resulted from the substitution of P, Si and Al.

Reference

[1] C. R. Shastry, J. J. Friel, and H. E. Townsend, ASTM STP 965 (Philadelphia, PA ASTM, 1988) p. 5.

[2] H. E. Townsend, and Z. C. Zoccola, ASTM 767 (Philadelphia, PA ASTM, 1988) p. 45.

[3] Sei J. Oh, Ph.D Thesis, Old Dominion University, Department of Physics (1997).

[4] C. P. Dillon, *Corrosion Control in the Chemical Process Industries* (Materials Technology Institute of the Chemical Process Industries, Inc., 1994).

[5] M. Yamashita, H. Miyuki, H. Nagano, and T. Misawa, Corro. Eng., **4**, 43(1994).

[6] T. Misawa, K. Asami, K. Hashimoto, and S. Shimodaira, Corr. Sci., **14**, 279(1974).

[7] I. Suzuki, and Y. Hisamatsu, J. Electrochem. Soc., **127(10)**, 2210(1980).

[8] M. Stratmann, K. Bohnenkamp, and T. Ramchandran, Corr. Sci., **27(9)**, 905(1987).

[9] H. Kihira, S. Ito, and T. Murata, Corr. Sci., **31**, 383(1990).

[10] A. Nishikayta, Y. Yamashita, H. Katayama, T. Tsuru, A. Usami, K. Tanabe, and Mabuchi, Corr. Sci., **37**, 2059(1995).

[11] M. Yamashita, and T. Misawa, Proc. 3rd NACE Am. Region Corr. Cong., Cancun Mexico (1998).

[12] H. Miyuki, Zairyo-to-Kankyo, **47**, 186(1998).

[13] S. J. Oh, S.-J. Kwon, D. C. Cook, and H. E. Townsend, Hyp. Int. C4, 37(1999).

[14] R. Balasubramanian, D. C. Cook, T. Perez, and J. Reyes, Hyp. Int. C4, 37(1999).

[15] M. Yamashita, H. Nagano, T. Misawa, and H. E. Townsend, ISIJ Int., **38**, 285(1998).

[16] E. Jackson, *Hydrometallurgical Extraction and Reclamation*, (John Willey & Sons., New York, 1986) p. 145.